The Astrophysical Journal Supplement Series, 169:472–484, 2007 April

THE SWAN SYSTEM OF C_2: A GLOBAL ANALYSIS OF FOURIER TRANSFORM EMISSION SPECTRA

A. Tanabashi,[1] T. Hirao,[2] and T. Amano[3]
Institute for Astrophysics and Planetary Sciences, Ibaraki University, Mito, Japan; tanabasia@riken.jp, tsuhirao@gmail.com, tamano@uwaterloo.ca

and

P. F. Bernath[4]
Department of Chemistry, University of Waterloo, ON, Canada; and Department of Chemistry, University of Arizona, Tucson, AZ; pfb500@york.ac.uk
Received 2006 October 4; accepted 2006 October 30

ABSTRACT

The C_2 Swan system ($d\,^3\Pi_g$-$a\,^3\Pi_u$) was observed in emission for the $\Delta v = -3$ to $\Delta v = +2$ sequences in the 14,000–24,000 cm^{-1} spectral range using a Fourier transform spectrometer. We carried out a global simultaneous fit by including a wide range of vibrational states. A total of 34 bands with $v' = 0$–10 and $v'' = 0$–9 were rotationally assigned. Numerous discrepancies were found in the assignments and in the measured transition wavenumbers between the new measurements and previous results. Most of the measured transition wavenumbers and their assignments for relatively low-v bands agreed with published data. On the contrary, for high-v bands our line positions and assignments disagreed with the tabulated literature values. In particular, the lines of six bands involving the levels with $v' = 4$, 5, and 6 are almost completely different from the previous work. Major sources of the disagreement are thought to be line congestion and perturbations found in these bands. From the analysis, perturbations for $v' = 0$, 1, 2, 4, 6, 8, 9, and 10 in the $d\,^3\Pi_g$ state were identified. A study of these rotational perturbations suggest that some of them are likely caused by interactions with high-v levels of the $b\,^3\Sigma_g^-$ state.

Subject headings: astrochemistry — ISM: clouds — ISM: molecules — methods: laboratory — molecular data — stars: late-type

Online material: extended figures, machine-readable table

1. INTRODUCTION

The C_2 molecule has been identified in a wide variety of astronomical objects such as the Sun (Grevesse & Sauval 1973; Lambert 1978; Brault et al. 1982), late-type stars (Querci et al. 1971; Goebel et al. 1983; Tautvaisiene et al. 2000; Reddy et al. 2002), interstellar molecular clouds (Souza & Lutz 1977; Chaffee & Lutz 1978; Hobbs 1979; Hobbs & Campbell 1982; Chafee et al. 1980; Hobbs 1981; van Dishoeck & de Zeeuw 1984; Hobbs et al. 1983; Federman & Huntress 1989; Sembach et al. 1996; Gredel 1999; Gredel et al. 2001; Cecchi-Pestellini & Dalgarno 2002), and comets (Mayer & O'Dell 1968; Lambert & Danks 1983; Johnson et al. 1983; Gredel et al. 1989; Fink & Hicks 1996). C_2 has also been the subject of extensive laboratory spectroscopic investigations (Huber & Herzberg 1979; Bernath & McLeod 2001). Huber & Herzberg (1979) tabulated the electronic, structural, and vibrational properties of C_2 as known up to about 1977. At present, to our knowledge, eleven low-lying electronic states of C_2 have been identified below 7 eV, and a triplet $c\,^3\Sigma_u^+$ state is thought to be located about 10,000 cm^{-1} above the ground state based on a perturbation analysis of the $A\,^1\Pi_u$ state (Ballik & Ramsay 1963a; Chauville et al. 1977; Davis et al. 1988), although no transitions from or to this state have been observed. Figure 1 summarizes the low-lying electronic states of C_2 and the observed transitions between them.

Of the nine observed systems of C_2, the most prominent bands in the visible region (~15,000–25,000 cm^{-1}) are the Swan system ($d\,^3\Pi_g$-$a\,^3\Pi_u$). The Swan system is easily excited in flames or discharges through gases containing carbon. Because this band system is so easily excited, it was believed that the $a\,^3\Pi_u$ state was the ground electronic state in the early studies. The history of Swan system observations can be traced back almost two centuries, and a comprehensive survey of the early historic work was given in a review by Tyte et al. (1967). Phillips & Davis (1968) observed the Swan system mainly in a carbon arc and compiled rotationally resolved transition wavenumbers for 35 bands with $v' = 0$–6 and 8–10 and $v'' = 0$–9. It should be emphasized that no transitions that involve the $v' = 7$ level were identified.

More recently, Amiot (1983) observed the (0, 0) band of the Swan system for the $^{12}C_2$, $^{13}C_2$, and $^{12}C^{13}C$ isotopologues using Fourier transform techniques. The (0, 1) and (1, 0) bands of $^{12}C_2$ were investigated by laser-induced fluorescence by Curtis & Sarre (1985) and Suzuki et al. (1985), respectively. They observed not only the regular transitions with $\Delta\Omega = 0$ but also a few cross transitions with $\Delta\Omega = \pm 1$. Prasad & Bernath (1994) recorded the low-v bands up to $v' = 3$ and $v'' = 4$ in emission with a Fourier transform spectrometer in a corona-excited supersonic jet expansion source and a hollow cathode discharge source. Recently, Lloyd & Ewart (1999) observed high-resolution spectra of the (0, 0) band using degenerate four-wave mixing. These investigations improved the accuracy of the line positions and molecular constants for some of the bands originally reported by Phillips & Davis. At first sight, therefore, all of the features of the Swan system seem to have been thoroughly investigated. However, the bands that involve high vibrational states for both the $a\,^3\Pi_u$ and $d\,^3\Pi_g$ states do not seem to be studied at high resolution with

[1] Present address: Terahertz Biological Sensing Research Laboratory, RIKEN, Saitama, Japan.
[2] Present address: Department of Chemistry, Okayama University, Japan.
[3] Present address: Department of Chemistry, University of Waterloo, ON, Canada.
[4] Also: Department of Chemistry, University of York, Heslington, York, UK.

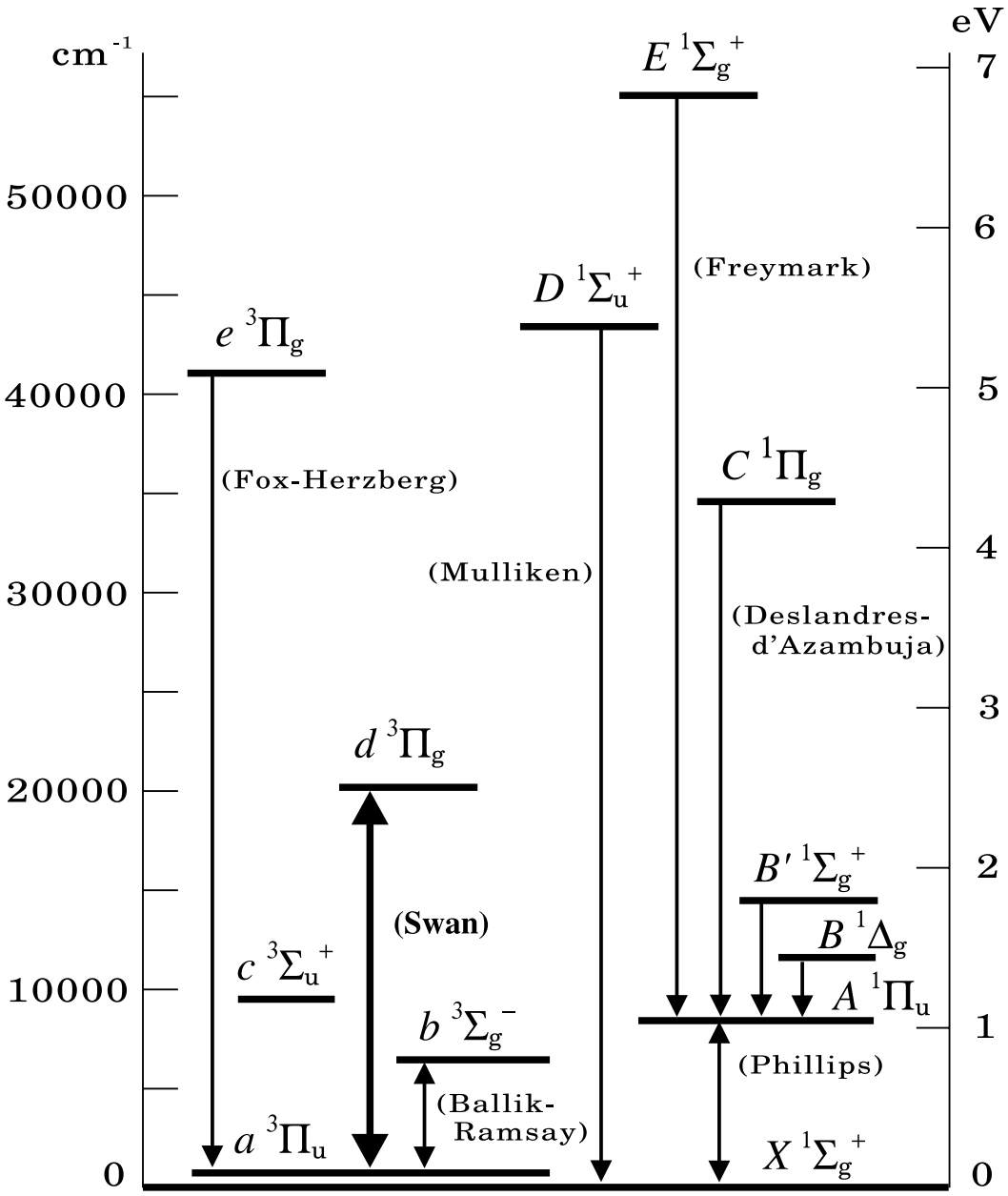

FIG. 1.—Low-lying electronic states of C_2. The direction of arrows indicates emission or absorption.

modern instrumentation and have not been analyzed systematically with global fitting programs.

As early as in 1910, Fowler (1910) found that the progression from the $v' = 6$ level appeared more intense than those from other vibrational levels in an electrical discharge through CO at a relatively high pressure of ~0.1 atm. This specific emission is sometimes called the "high-pressure bands," even though, later, they were found to be produced at much lower pressures under a variety of experimental conditions (Little & Browne 1987; Weltner & Van Zee 1989). Several mechanisms have been proposed for this abnormal enhancement of the intensity of transitions from $v' = 6$ (Herzberg 1946; Setser & Thrush 1963; Savadatti & Broida 1966; Kunz et al. 1967; Little & Browne 1987; Caubet & Dorthe 1994; Erman 1980).

Tanabashi & Amano (2002) observed three bands of the Swan system by a direct absorption technique using a tunable dye laser as a radiation source. In their study, they found a new band that was assigned as (7, 9) as well as two known bands that were assigned as (6, 8) and (5, 7). The only available analysis for such high-v levels of the $d\,^3\Pi_g$-$a\,^3\Pi_u$ system was published by Phillips & Davis (1968). However, the newly observed absorption spectra of the (6, 8) and (5, 7) bands were found not to agree with those identified by Phillips & Davis (1968). We correctly identified bands that involved the $v' = 6$ state in $d\,^3\Pi_g$ and revealed that this state was not particularly different from other states. Therefore, the mechanisms proposed to explain the "high-pressure" bands were in retrospect made based on a set of incorrect spectroscopic constants.

To sort out the discrepancies with previous work, we undertook a thorough investigation of the entire Swan band system. These new measurements were carried out with a high-resolution Fourier transform spectrometer (Bruker IFS 120 HR) at the University of Waterloo in Canada. The C_2 molecule was produced in a microwave discharge through a mixture of acetylene and argon, and the Swan system was observed in emission. Spectra were recorded to cover the 14,000–24,000 cm^{-1} range at a resolution of

0.10 cm^{-1}. The increased resolution associated with the Fourier transform spectrometer (FTS) permitted the identification of 34 bands up to the (10, 9) band. We also identified the $v' = 7$ level through the observation of the (7, 6) and (7, 9) bands and confirmed that this new level is indeed a member of the Swan system. A total of 30 bands spanning $v' = 0$–10 and $v'' = 0$–9 were rotationally analyzed simultaneously.

We confirmed the measured transition wavenumbers and the assignments obtained from the dye laser absorption spectra (Tanabashi & Amano 2002), and moreover, we found that such discrepancies existed over a wider range. Most of the measured transition wavenumbers and the line assignments in our FT spectra for relatively low-v bands were found to agree with the data published by Phillips & Davis (1968). However, for the high-v bands the new line assignments in many cases do not agree with the tabulated literature values. In particular, our line assignments and transition wavenumbers for the six bands involving the levels of $v' = 4$, 5, 6 are almost completely different from the earlier ones. Major sources of this disagreement are probably caused by heavy line congestion and small but numerous perturbations. From the analysis, perturbations were found in the upper $d\ ^3\Pi_g$ state for $v' = 0$, 1, 2, 4, 6, 8, 9, and 10. A study of these rotational perturbations suggests that some of them are the result of interactions with the high-v levels of the $b\ ^3\Sigma_g^-$ state. However, details of the perturbations are not completely understood and remain a subject of further investigation. We intend to carry out a more detailed analysis in the future.

2. EXPERIMENTAL PROCEDURE

The Swan system was observed in emission from a microwave discharge in a flow of acetylene (C_2H_2) diluted in argon through a discharge tube. An Evenson-Broida microwave cavity was attached to the center of a glass cell (~15 cm long) and 80 W of power was applied at a frequency of 2450 MHz. The partial pressure of acetylene was a few tens of mtorr, and the total pressure was about 2 torr. The discharge glow was focused onto the Fourier transform spectrometer (FTS) emission port with a CaF_2 lens.

Because we did not evacuate the spectrometer, we have converted the "air" wavenumbers to vacuum wavenumbers with our usual procedure (Hirao et al. 2000). To reduce the influence of strong transitions of other molecules and atoms, several optical filters were used. Two sets of spectra were recorded to cover the range from 14,000 to 24,000 cm^{-1}. The first covered the range from 15,800 to 24,000 cm^{-1} with a 400 nm red-pass filter and a 600 nm blue-pass filter. This region contained the $\Delta v = -2, -1, 0, +1$, and +2 sequences and some bands of the $A\ ^2\Delta$-$X^2\Pi$ system of CH. The second region covered the 14,000 to 17,100 cm^{-1} spectral range with a 588 nm red-pass filter and a 700 nm blue-pass filter, and we used a notch filter to attenuate the strong He-Ne laser line at 632.8 nm. In this range, the spectra of $\Delta v = -2$ and the weaker $\Delta v = -3$ sequences were recorded. To obtain a good signal-to-noise ratio, the emission spectra were accumulated over 50 scans at a spectral resolution of 0.10 cm^{-1}. The observed line width of C_2 was about 0.15 cm^{-1}. The C_2 line widths did not change when we increased the resolution, indicating that, because of the high plasma temperature of the discharge, the line widths were primarily determined by the Doppler effect. The observed line width is consistent with a translational temperature of about 2700 K.

The transition wavenumbers were measured using a Windows-based program called WSpectra, written by Michel Carleer (Laboratoire Chimie Physique Moléculaire, Université Libre de Bruxelles, Belgium) and calibrated against argon atomic lines observed at the same time. The calibration factors were obtained for the two sets of spectra as 1.00000212 (blue region) and 1.00000240 (red region) on the basis of standard Ar atomic lines (Norlen 1973). The precision of the transition wavenumbers was estimated to be 0.005 cm^{-1} for clear unblended lines. However, many lines are overlapped in very congested regions and the measurement precision is often degraded. The estimated uncertainties of transition wavenumbers for the blended lines range from 0.01 to 0.15 cm^{-1}.

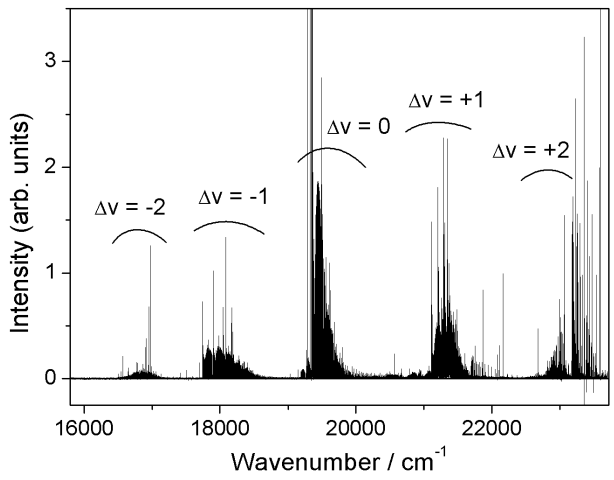

FIG. 2.—Overview of the observed spectra. The most intense lines around 19,300 cm^{-1} are due to Ar atomic lines.

3. OBSERVED VIBRATIONAL BANDS

In this investigation, the Swan system was observed up to $v' = 10$ for the upper state and $v'' = 9$ for the lower state in emission. A total of 34 bands belonging to the $\Delta v = -3$ to +2 sequences were identified. An overview of the observed spectra is shown in Figure 2. Each sequence contains several closely spaced bands, so the spectra have a very complicated appearance with many lines from different bands piled up in the same region. For each band three *P* branches and three *R* branches were identified. The rotational analysis could be carried out for relatively high levels up to about $J' = 85$ and $J' = 60$ for bands with $v' = 0$ and $v' = 1$, respectively. For the vibrational levels with $v' = 2$–10, the rotational assignments could be made for J up to 30–50. All the band heads of the rotationally analyzed bands are listed in Table 1.

A sizable portion of the observed bands were found to be perturbed, as will be discussed below, and this was another source of difficulty in assigning the lines. To unravel the perturbations, a simultaneous analysis of several vibrational bands that shared a common vibrational level was carried out. Reasonable and consistent assignments were reached for 30 bands by trial and error.

3.1. *The* $\Delta v = +1$ *Sequence*

The $\Delta v = +1$ sequence is the most extensive one in the Swan system. This sequence is located in the wavenumber region between 20,800 and 21,700 cm^{-1}. The overall picture of this sequence is shown in Figure 3. Although the line density was generally high, as shown in this figure, the identification of lines was not difficult, as long as they were free from severe overlaps. The first member of the sequence, the (1, 0) band, forms a band head at 21,104 cm^{-1} and is followed by the (2, 1), (3, 2), . . . , up to (10, 9) bands. Figure 4 shows a part of the *R* branch lines of the (1, 0) band. A distinctive pattern of triplets can be easily traced. The assignments of the (1, 0) band by Phillips & Davis

TABLE 1
HEADS OF OBSERVED BANDS

v'	v''	$\tilde{\nu}$ (cm^{-1})
3	6	15149.182
0	2	16147.297
3	5	16648.361
4	6	16777.380
5	7	16877.390
6	8	16946.214
7	9	16969.830
0	1	17739.749
1	2	17898.573
2	3	18043.263
3	4	18170.342
4	5	18275.753
5	6	18353.387
0	0	19354.781
1	1	19490.226
2	2	19611.372
3	3	19714.855
1	0	21104.144
2	1	21201.680
3	2	21281.549
4	3	21338.909
5	4	21368.012
6	5	21360.017
7	6	No heads[a]
8	7	No heads[a]
9	8	No heads[a]
10	9	20958.384[b]
2	0	22813.757
3	1	22869.289
8	6	No heads[a]

[a] No head appears in the range of observed lines.
[b] The head appears in the R branch in contrast to the other bands, which have P-branch heads.

(1968) are indicated at the top of the figure by short vertical lines, and our assignments are shown at the bottom. The assignments and the measured transition wavenumbers of the two sets of data agree reasonably well.

The assignments of lines in the congested region were made step by step, starting from the (1, 0) band and then going to higher

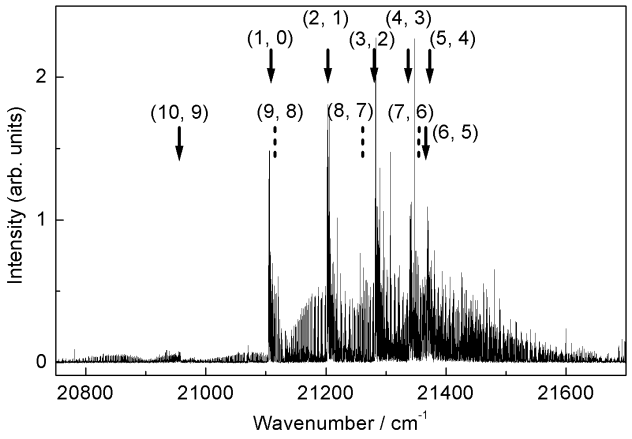

FIG. 3.—Sequence $\Delta v = +1$. Arrows indicate the band head positions for each band, and short dashed lines indicate the band origins for (9, 8), (8, 7), and (7, 6) bands, which have no band heads.

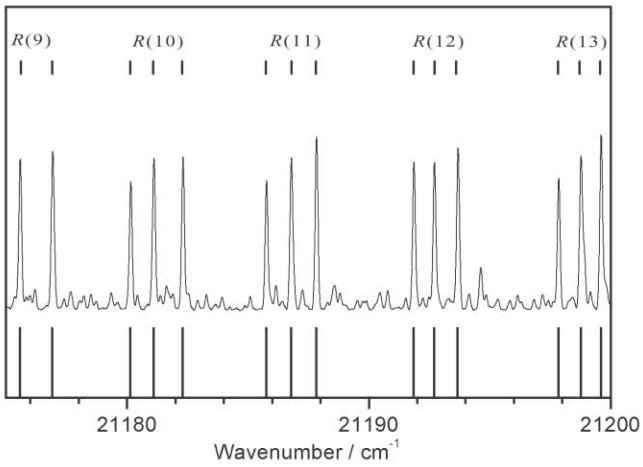

FIG. 4.—Section of the (1, 0) band. The triplet pattern of the R-branch lines are clearly seen. Here the rotational quantum numbers N are used rather than J. The assigned line positions by Phillips & Davis (1968) are given at the top, and our assignments are at the bottom. No major discrepancies are found between the two sets of assignments.

vibrational bands. The transitions of the next low-v band, i.e., (2, 1), were thus assigned after the (1, 0) band lines were sorted out, and a similar process was repeated for higher vibrational bands until almost all prominent lines were assigned. The band head positions for the (2, 1), (3, 2), (4, 3), and (5, 4) bands are 21,202, 21,282, 21,339, and 21,368 cm^{-1}, respectively. The separation between these values decreases as v increases, and they form a head of heads. The band head of the (6, 5) band turns around and is located at 21,360 cm^{-1}, lower than that of the (5, 4) band. As a result, the line density becomes very high in the 21,400 to 21,600 cm^{-1} region. Several hundred lines pile up and a part of this region is shown in Figure 5. The assigned line positions by Phillips & Davis (1968) are given at the top of this figure, and our assignments are at the bottom. These two sets of assignments do not agree.

It is useful to make a critical comparisons between our new results and the previous work of Phillips & Davis (1968). For the (1, 0) and (2, 1) bands, our assignments are consistent with those of Phillips & Davis (1968). The (3, 2) band has been unambiguously assigned up to $J \sim 30$ in this investigation, while Phillips & Davis (1968) identified a limited number of high-J transitions. For the (4, 3) band, the identification and the assignments by Phillips & Davis (1968) were found to be problematic, e.g., some of the lines of one of the three spin components are misassigned to an unrelated band. The (5, 4) and (6, 5) bands appear in the same wavenumber region almost on top of each other, as shown in Figure 3. Most line assignments for the (5, 4) and (6, 5) bands by Phillips & Davis (1968) turned out to be incorrect, and the assignments and the transition wavenumbers obtained by us are listed in Table 7 in Appendix A. The higher vibrational bands, (7, 6), (8, 7), and (9, 8), with band origins located at 21,360, 21,260, and 21,100 cm^{-1}, respectively, were also identified. These three bands form no band heads within the observed range of the J values, and these bands are often referred to as "headless bands." The (7, 6) and (8, 7) bands were identified for the first time by this investigation. The (9, 8) and (10, 9) bands are well isolated from other bands, and they are easily identified in contrast to the lower v bands in the congested region. Phillips & Davis (1968) also identified these two bands, and their assignments agree with ours. The (10, 9) band forms a band head in the R branch at 20,958 cm^{-1} and is therefore red degraded in contrast to other blue degraded bands of the Swan system. The degree of disagreements in the

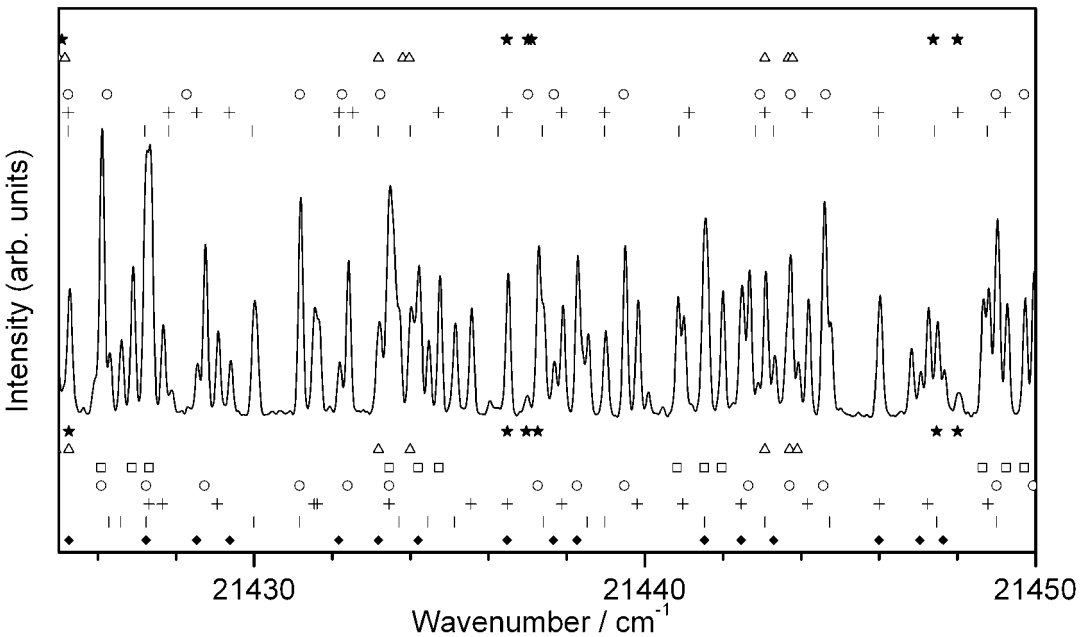

FIG. 5.—Example of a very congested region of the spectrum. The assigned line positions by Phillips & Davis (1968) are given at the top, and our assignments are at the bottom. Several bands are overlapped, and the symbols distinguish the transitions of (1, 0) (*stars*), (2, 1) (*triangles*), (3, 2) (*squares*), (4, 3) (*circles*), (5, 4) (*pluses*), (6, 5) (*short vertical lines*), and (7, 6) (*diamonds*). The two sets of assignments disagree in many cases for the higher v bands.

assignments between the work of Phillips & Davis (1968) and ours are summarized in Table 2.

3.2. *The* $\Delta v = 0$ *Sequence*

The $\Delta v = 0$ sequence is located in the 19,350 to 19,950 cm^{-1} region. The (0, 0) band was the strongest band in our spectrum, and the (1, 1) band was much weaker. The intensity of the succeeding bands rapidly diminished. We identified bands in this sequence up to the (3, 3) band. The (4, 4) band was too weak to make a reliable analysis. The (0, 0) band forms a band head at 19,354 cm^{-1} in the P branch. The (1, 1), (2, 2), and (3, 3) bands have band heads at 19,490, 19,611 and 19,715 cm^{-1}, respectively, as listed in Table 1. They are all blue degraded as are most other bands.

3.3. *The* $\Delta v = -1$ *Sequence*

The $\Delta v = -1$ sequence, the (0, 1), (1, 2), (2, 3), (3, 4), (4, 5), and (5, 6) bands, lies in the 17,740–18,600 cm^{-1} range. They are all blue degraded and have a single head in the P branch. These bands are relatively well separated from each other, and there is no head of heads in contrast to the $\Delta v = +1$ sequence. Phillips & Davis (1968) also observed these six bands and their band head positions were at 17,739.73, 17,898.57, 18,043.25, 18,170.40, 18,275.59, and 18,351.36 cm^{-1} for the bands from (0, 1) to (5, 6), respectively. Our band head positions are listed in Table 1, and a comparison reveals that the lower vibrational bands up to (3, 4) are consistent. For these four bands [i.e., (0, 1) to (3, 4)] the assignments and transition wavenumbers obtained by Phillips & Davis (1968) are in good agreement with our results. However, the band head position for the (4, 5) band is different, and the line assignments by Phillips & Davis (1968) mostly disagree with ours. For the (5, 6) band, the difference in the band head position is about 2 cm^{-1}, and their line positions for the entire band seem to be shifted to lower wavenumbers as compared to ours. The differences, however, are not just shifts: the line assignments are completely different. We encountered a similar situation in the bands associated with $v' = 4,\ 5,\ 6$ in other sequences, for which previous rotational assignments are wrong.

TABLE 2

COMPARISON OF THE ASSIGNMENTS

v''/v'	0	1	2	3	4	5	6	7	8	9	10
0	○	○	○								
1	○	○	○	○							
2	○	○	○	○							
3		○	○	○	△						
4		○	○	○		×					
5			○	○	△		×				
6				○	×	×		□	○		
7						×			□		
8							×			○	
9								□			○

NOTES.—The observed bands are indicated by symbols. Each symbol indicates the degree of agreement between our assignments and those of Phillips & Davis: *circles*, 80%–100%; *triangles*, 20%–80%; *crosses*, 0%–20%; and the newly identified bands are indicated by a square.

3.4. *The* $\Delta v = -2$ *Sequence*

The (0, 2), (1, 3), (2, 4), . . . , and (7, 9) bands have been recorded in the region between 16,150 and 17,100 cm^{-1}. The low-v bands in this sequence are well separated, but the higher v bands become congested, making the assignments more difficult. Among these, the (5, 7), (6, 8), and (7, 9) bands were observed in absorption by using a dye laser as a radiation source (Tanabashi & Amano 2002). The (7, 9) band was identified for the first time by the absorption spectroscopy (Tanabashi & Amano 2002). Moreover, Tanabashi & Amano (2002) discovered that the measured transition wavenumbers and the assignments by Phillips & Davis (1968) for the (5, 7) and (6, 8) bands were not correct as discussed in their paper (Tanabashi & Amano 2002). These three bands have also been identified in the emission spectra, and the measured transition wavenumbers and the assignments are in good agreement

TABLE 3
MOLECULAR CONSTANTS FOR THE $a\ ^3\Pi_u$ STATE (IN cm^{-1})

v	T_v	A	A_D	B	$D \times 10^6$	λ	o	p	q
0[a]	0	−15.26912 (20)	0.0002388 (33)	1.6240451 (22)	6.45068 (84)	−0.15490 (25)	0.67539 (20)	0.002465 (24)	−0.0005319 (20)
1.....	1618.02330 (31)	−15.25176 (27)	0.0002029 (32)	1.6074301 (20)	6.44478 (84)	−0.15355 (21)	0.66997 (21)	0.002697 (20)	−0.0005779 (18)
2.....	3212.72262 (41)	−15.23388 (63)	0.0001684 (41)	1.5907615 (27)	6.4581 (18)	−0.15206 (50)	0.66308 (57)	0.003068 (33)	−0.0006472 (21)
3.....	4784.1113 (31)	−15.2262 (52)	0.000106 (21)	1.574009 (12)	6.4573 (95)	−0.1592 (44)	0.6496 (44)	0.00352 (21)	−0.0007679 (76)
4.....	6332.1373 (22)	−15.2031 (30)	0.000185 (17)	1.557175 (14)	6.444 (17)	−0.1448 (33)	0.6504 (30)	0.00527 (17)	−0.0008912 (71)
5.....	7856.8242 (17)	−15.2009 (25)	0.000005 (13)	1.540145 (11)	6.349 (15)	−0.1443 (23)	0.6394 (20)	0.00646 (12)	−0.0012316 (55)
6.....	9358.1728 (23)	−15.1586 (36)	0.000226 (17)	1.523437 (14)	6.101 (19)	−0.1416 (27)	0.6491 (28)	0.00403 (16)	−0.0006443 (73)
7.....	10836.1550 (45)	−15.0856 (64)	0.00046 (15)	1.50875 (12)	3.05 (39)	−0.1478 (48)	0.6538 (65)	−0.0283 (14)	0.00685 (26)
8.....	12290.903 (27)	−15.247 (57)	−0.00006 (10)	1.48789 (18)	3.71 (12)	−0.082 (36)	0.735 (43)	0.0033 (31)	−0.00202 (19)
9.....	13722.1096 (33)	−15.0808 (53)	0.000482 (24)	1.472691 (21)	5.793 (40)	−0.1662 (20)	0.6516 (43)	0.00296 (32)	−0.000207 (18)

NOTE.—The numbers in parentheses indicate 1 standard deviation to the last significant digits of the constants.
[a] To fit the $v = 0$ data higher order terms were needed and were determined to be $H = 6.745\ (77) \times 10^{-12}$, $o_D = -7.87\ (58) \times 10^{-6}$, $p_D = 0.063\ (14) \times 10^{-6}$, and $q_D = -0.00950\ (26) \times 10^{-6}$.

with the results obtained by absorption spectroscopy. Those data from the absorption spectroscopy together with some additional lines mostly for high-J transitions were included in the least-squares analysis.

3.5. *The $\Delta v = -3$ Sequence*

The wavenumber range of 14,000–17,000 cm^{-1} was recorded in a separate experiment. The (1, 4), (2, 5), (3, 6), and (4, 7) bands were identified in the range from 14,550 to 15,400 cm^{-1}. Unfortunately, the notch filter used to block the He-Ne metrology laser also attenuated the high wavenumber side of the (4, 7) band and the entire region where the (5, 8) and higher vibrational bands are expected.

3.6. *The $\Delta v = +2$ Sequence*

The $\Delta v = +2$ sequence was observed in the range of 22,600–23,100 cm^{-1}. Strong lines of the $A\ ^2\Delta$-$X\ ^2\Pi$ system of CH also appeared in this region, and covered the weaker C_2 spectra under our experimental conditions; only the (2, 0), (3, 1), and (8, 6) bands were rotationally analyzed. The bands from (4, 2) to (7, 5) were difficult to analyze because they were weak in intensity and the lines were heavily overlapped due to the formation of a head of heads. The (2, 0) and (3, 1) bands have P-branch heads at 22,814 and 22,869 cm^{-1}, respectively, and the (8, 6) band is a headless band with the band origin located at 22,744 cm^{-1}. Band heads can be identified at 22,902 and 22,904 cm^{-1} for the (4, 2) and (5, 3) bands, as expected by calculation.

4. ANALYSIS AND DISCUSSION

4.1. *A Global Fit*

An iterative, nonlinear, weighted least-squares fitting program was used for analysis of the measured wavenumbers for more than 3400 transitions. The transition wavenumbers for all the identified bands were fitted together, and a set of 187 parameters were determined. All the transition wavenumbers and rotational assignments determined in this work are listed in Appendix A.

The effective Hamiltonian of Brown and Merer for a $^3\Pi$ state was used for the analysis (Brown & Merer 1979). Known high-resolution data obtained by Curtis & Sarre (1985) for the (0, 1) band, by Suzuki et al. (1985) for the (1, 0) band, and by Prasad & Bernath (1994) for the bands up to (3, 4) were included in the fit to improve the constants for the low-v states. Curtis & Sarre (1985) and Suzuki et al. (1985) observed several "cross transitions" between the $F_1 \leftrightarrow F_2$, $F_2 \leftrightarrow F_1$, $F_2 \leftrightarrow F_3$, and $F_3 \leftrightarrow F_2$ spin components. These lines are useful in determining more accurate spin-orbit coupling constants and Λ-doubling parameters. In the fitting, each input data point was weighted by the square of the reciprocal of its estimated uncertainty of the measurements: $w_i = (\delta\nu_i)^{-2}$. The uncertainty ($\delta\nu_i$) was determined for each line on the basis of the signal-to-noise ratio and the line width. However, in many cases the spectral lines are broadened because of overlaps of several transitions. The transition wavenumbers for blended lines were included in the fit with reduced weights, depending on the uncertainties, ranging from 0.01 to 0.10 cm^{-1}. Perturbed lines were mostly excluded from the fit. The vibrational levels with $v = 4$, 6, and 9 of the $d\ ^3\Pi_g$ state were affected by perturbation over almost the entire range of observed rotational levels. In order to determine approximate spectroscopic parameters, these data were included in the fit with reduced weights of up to 1/400 of those for clear unblended lines. It was also necessary to fix certain parameters to obtain a reasonable fit. The A_D and D values for $v = 6$ of the $d\ ^3\Pi_g$ state were fixed to estimated values calculated from other vibrational levels. Similarly, for the $v = 8$, 9, and 10 levels, the A_D parameters were also fixed. However, it was difficult to judge which line should be included in the fit with what weight for the bands that were entirely affected by perturbations as in the case of the (6, 8) band observed by a dye laser absorption spectroscopy (Tanabashi & Amano 2002). After many trials, rough values for the spectroscopic constants were derived for these heavily perturbed vibrational levels (e.g., $v = 4$, 6) of the $d\ ^3\Pi_g$ state.

The molecular constants determined from the least-squares fit are summarized in Tables 3 and 4 for the $a\ ^3\Pi_u$ and $d\ ^3\Pi_g$ states, respectively. Major constants such as the rotational constants and the spin-orbit coupling constants show a reasonable smooth vibrational dependence, while some irregularities are noticeable in minor constants such as the spin-spin and Λ-type doubling parameters. The term energy was given relative to the origin of the $v = 0$ state of $a\ ^3\Pi_u$. If absolute energies are needed relative to the ground state, the energy difference between the origin of the $v = 0$ of the $a\ ^3\Pi_u$ state and the origin of the ground state $X\ ^1\Sigma_g^+$ should be added. This difference has been determined to be 1536.0731 cm^{-1} from a perturbation analysis by Amiot et al. (1979), although this value needs to be used with caution because a different formulation of the effective Hamiltonian was used.

From the laser absorption spectrum recorded by Tanabashi & Amano (2002) the molecular constants for the $v = 5$, 6, 7 states in $d\ ^3\Pi_g$ and for the $v = 7$, 8, 9 states in $a\ ^3\Pi_u$ were determined. Tanabashi & Amano corrected the assignments made by Phillips & Davis and eliminated an abnormality in the vibrational dependence

TABLE 4
MOLECULAR CONSTANTS FOR THE $d\ ^3\Pi_g$ STATE (IN cm^{-1})

v	T_v	A	A_D	B	$D\times10^6$	λ	o	p	q
0.....	19378.46446 (30)	−14.00111 (28)	0.0004803 (37)	1.7455695 (20)	6.82103 (66)	0.03303 (20)	0.61085 (22)	0.003947 (20)	−0.0007762 (18)
1.....	21132.13960 (13)	−13.87440 (24)	0.0005495 (43)	1.7254012 (25)	6.9647 (13)	0.03018 (27)	0.61703 (21)	0.004181 (25)	−0.0008310 (22)
2.....	22848.4150 (30)	−13.8444 (49)	0.000655 (23)	1.704494 (13)	7.360 (11)	0.0108 (43)	0.6205 (43)	0.00431 (20)	−0.0009841 (69)
3.....	24524.2222 (11)	−13.5329 (18)	0.000637 (11)	1.6814609 (79)	7.490 (11)	0.0515 (15)	0.5724 (14)	0.005213 (85)	−0.0008519 (40)
4.....	26155.0003 (49)	−13.3557 (89)	0.000621 (28)	1.657484 (17)	8.095 (12)	0.0448 (55)	0.5382 (60)	0.00439 (23)	−0.0010884 (82)
5.....	27735.6847 (26)	−13.0264 (47)	0.000582 (22)	1.630248 (15)	8.694 (18)	0.0823 (29)	0.5633 (32)	0.00541 (18)	−0.0008693 (70)
6.....	29259.704 (14)	−13.082 (35)	0.00052 (fixed)	1.599841 (19)	9.0 (fixed)	0.062 (14)	0.559 (16)	0.00104 (65)	−0.001514 (17)
7.....	30717.9217 (33)	−12.3299 (58)	0.000903 (28)	1.565922 (22)	9.787 (42)	0.0901 (20)	0.5127 (43)	0.00901 (30)	−0.001283 (15)
8.....	32102.6713 (90)	−12.0890 (95)	0.00052 (fixed)	1.52672 (12)	9.58 (39)	0.046 (12)	0.4915 (96)	0.00457 (84)	−0.000863 (84)
9.....	33406.325 (28)	−11.785 (66)	0.00052 (fixed)	1.48487 (18)	10.04 (14)	0.232 (43)	0.564 (49)	−0.0014 (28)	−0.00201 (20)
10.....	34626.8093 (47)	−11.2469 (79)	0.00052 (fixed)	1.440994 (34)	12.544 (48)	0.1162 (65)	0.3578 (64)	0.00702 (47)	−0.001119 (20)

NOTE.—The numbers in parentheses indicate 1 standard deviation to the last significant digits of the constants.

of the rotational constants, as shown in Figure 5 of Tanabashi & Amano (2002). Comparison between the new set of parameters and those obtained in Tanabashi & Amano (2002) reveals slight differences. The new constants obtained in this investigation are thought to be more accurate, as the analysis was carried out by including all the available data simultaneously.

The spectroscopic parameters of Tables 3 and 4 were used to derive the equilibrium molecular constants for the vibrational, the rotational, and the spin-orbit coupling constants by using customary energy level expressions for a vibrating rotator

$$G(v) = \omega_e\left(v+\frac{1}{2}\right) - \omega_e x_e\left(v+\frac{1}{2}\right)^2 + \omega_e y_e\left(v+\frac{1}{2}\right)^3 + \omega_e z_e\left(v+\frac{1}{2}\right)^4, \quad (1)$$

$$B_v = B_e - \alpha_e\left(v+\frac{1}{2}\right) + \gamma_e\left(v+\frac{1}{2}\right)^2 + \delta_e\left(v+\frac{1}{2}\right)^3, \quad (2)$$

$$A_v = A_e + \alpha_e^A\left(v+\frac{1}{2}\right) + \gamma_e^A\left(v+\frac{1}{2}\right)^2, \quad (3)$$

for the $a\ ^3\Pi_u$ and $d\ ^3\Pi_g$ states, and the values obtained are listed in Table 5. Extensive perturbations in the $d\ ^3\Pi_g$ state make it difficult to determine all the $G(v)$ values for the levels up to the $v = 10$ to the accuracy expected from the experimental precision. Therefore, relatively unperturbed levels were used to obtain a reasonable fit. As a result, ω_e, $\omega_e x_e$, $\omega_e y_e$, nd $\omega_e z_e$ were determined by using the data of $v = 1$, 2, 3, 5, 7, and 8 for the $d\ ^3\Pi_g$ state. The $\omega_e z_e$ term was not significant for the lower $a\ ^3\Pi_u$ state. The equilibrium internuclear distances r_e of 1.311946(16) and 1.265122(32) Å for the $a^3\ \Pi_u$ and $d\ ^3\Pi_g$ states, respectively, have been derived from the B_e values without correcting for the effect of the breakdown of the Born-Oppenheimer approximation such as the second-order contribution to the rotational energy from the electron-rotation interaction. Although the constants for the $a\ ^3\Pi_u$ state were determined with better precision by Amiot et al. (1979), the values obtained here are probably more realistic because our analysis involved a wider range of v.

TABLE 5
EQUILIBRIUM CONSTANTS (IN cm^{-1})

Constants	$a\ ^3\Pi_u$	$d\ ^3\Pi_g$
ω_e.....	1641.341 (23)[a]	1789.094 (21)[b]
$\omega_e x_e$.....	11.6580 (58)	17.367 (15)[b]
$\omega_e y_e$.....	−0.00083 (41)	−0.1360 (36)[b]
$\omega_e z_e$.....	...	−0.04878 (25)[b]
B_e.....	1.63235 (4)	1.75542 (9)
α_e.....	0.01657 (3)	0.0196 (1)
γ_e.....	−0.000027 (5)	−0.00013 (4)
δ_e.....	...	−0.000082 (3)
r_e (Å).....	1.311946 (16)	1.265122 (32)
A_e.....	−15.2770 (3)	−14.0507 (5)
α_e^A.....	0.0160 (4)	0.0916 (5)
γ_e^A.....	0.00036 (7)	0.01693 (8)

[a] The numbers in parentheses indicate one standard deviation to the last significant digits of the constants.
[b] These values were obtained using the data only of $v = 1, 2, 3, 5, 7$, and 8 that are relatively unperturbed. See text for details.

4.2. *The Rotational Perturbations*

It is well known that the Swan system exhibits numerous, but relatively small, perturbations (Callomon & Gilby 1963; Phillips 1968). Callomon & Gilby identified perturbations in the $v = 0$, 1, and 2 levels in the $d\ ^3\Pi_g$ state. Their analysis suggested that the perturbations in these vibrational levels were caused by the interaction with $v = 11$–16 vibrational levels in the $b\ ^3\Sigma_g^-$ state (Callomon & Gilby 1963). The rotational term values for these high-v energy levels of the $b\ ^3\Sigma_g^-$ state were extrapolated from lower v states observed by Ballik & Ramsay (1963b). The Callomon & Gilby spectra had a rather high rotational temperature, so the perturbations they observed involved high-J lines, while Phillips (1968) identified perturbations with lower J rotational states. In addition, Phillips reported the identification of perturbations in the $v' = 3$, 4, and 5 levels. The majority of these perturbations were ascribed to the $b\ ^3\Sigma_g^-$ state. He suggested that the $X\ ^1\Sigma_g^+$ state was involved in some of the perturbations, but later Amiot (1983) concluded that the $X\ ^1\Sigma_g^+$ state was not involved in perturbing the $d\ ^3\Pi_g$ state, at least for the $v = 0$ level based on studies using the isotopic species $^{13}C_2$ and $^{12}C^{13}C$.

Our observation reproduced most of the perturbations identified previously for the low-v states (Callomon & Gilby 1963; Phillips 1968). Callomon & Gilby (1963) proposed that the perturbation involving the $F_2(51)$ level in the $v = 0$ state was caused by a $^1\Delta_g$ state that was unobserved at that time. This $^1\Delta_g$ state was later detected by Fourier transform emission spectroscopy by Douay et al. (1988). We confirm that this level is perturbed.

Callomon & Gilby (1963) pointed out that the perturbation of the $N = 47$ level in $d\ ^3\Pi_g\ v' = 0$ was caused by an almost exact resonance with the $N = 47$ rotational level of the $b\ ^3\Sigma_g^-$ state.

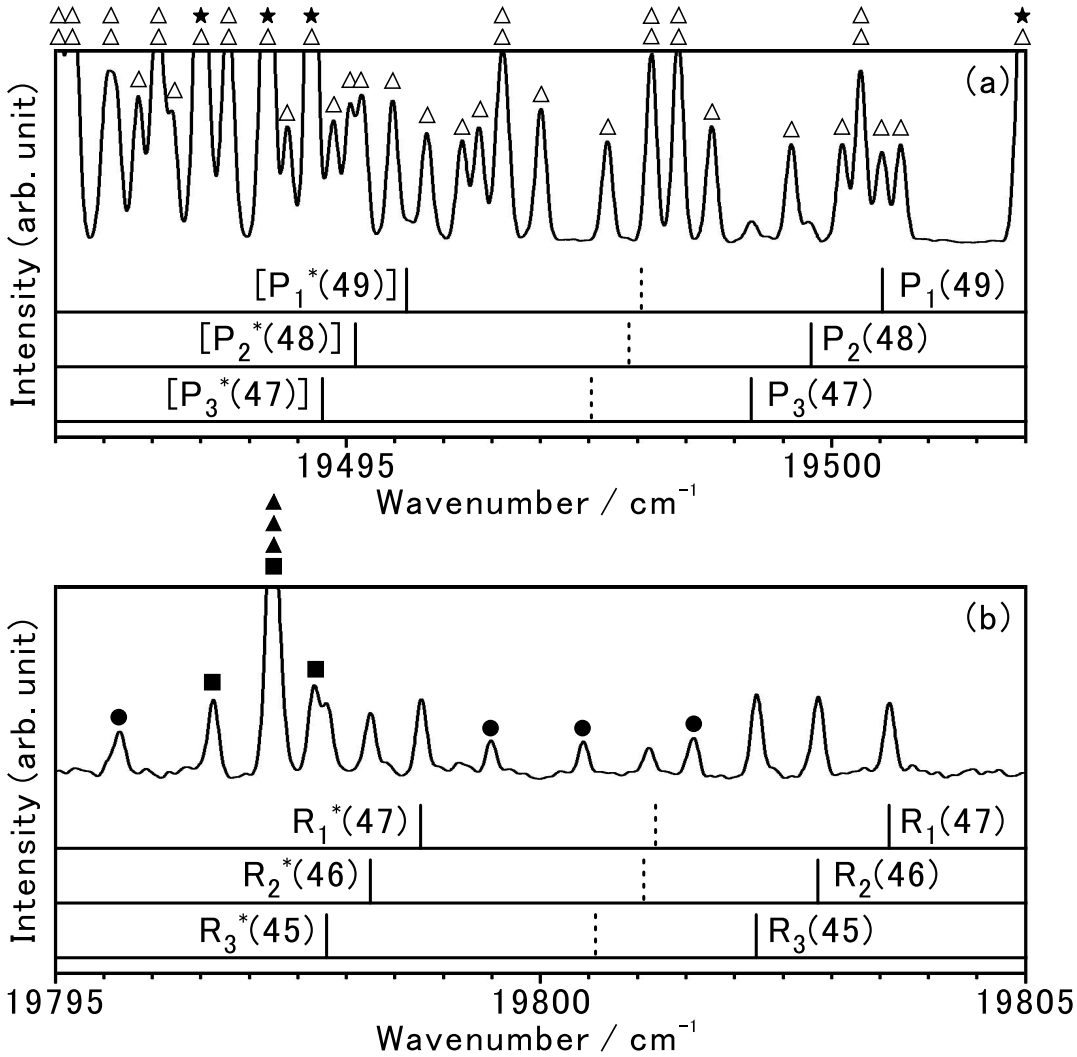

FIG. 6.— Sections of (*a*) *P*-branch and (*b*) *R*-branch regions of the (0, 0) band. Stars, triangles, squares, and circles indicate the (0, 0), (1, 1), (2, 2), and (3, 3) band lines, respectively. The open and filled symbols represent the *P* and *R* branches, respectively. The expected line positions for (*a*) the $P_1(49)$, $P_2(48)$, $P_3(47)$ transitions and for (*b*) the $R_1(47)$, $R_2(46)$, and $R_3(45)$ are indicated by dashed vertical lines. No lines are observed at those expected positions. Instead, the lines are identified at higher wavenumber by about 1.5 cm^{-1} than the corresponding unperturbed line positions. Note that some extra transitions around 19,798 cm^{-1}, which are marked by asterisks (*), are likely to be the transitions from the perturbing state.

Phillips (1968) listed in his Table III the shifts for the $N = 47$ rotational levels [$F_1(48)$, $F_2(47)$, and $F_3(46)$]. According to their analysis, this is one of the most conspicuous perturbations in the Swan system. Figure 6 displays the perturbed lines together with the extra perturbing lines. This figure corresponds to Figures 1*a*, 1*b*, and 1*d* of Callomon & Gilby (1963) but at higher resolution. The density of lines in the *R*-branch region is not high and the assignments of the perturbed *R*-branch lines is straightforward, and the extra lines identified by Callomon & Gilby (1963) are indeed confidently identifiable. These lines are marked by asterisks (*) in Figure 6. Based on the *R*-branch assignments, the *P* branches can be predicted. However, the line density in the *P*-branch region is much higher and the extra lines listed by Callomon & Gilby (1963) are buried under stronger lines, and their identification cannot be made with confidence, as Figure 6 indicates. Evidently, the spectrum obtained by Callomon & Gilby (1963) is simpler without much overlap with other bands. As all the three fine-structure components ($J = 46$, 47, and 48) are perturbed with a similar magnitude, the perturbing state is very likely to be the $N = 47$ level of the $b\ ^3\Sigma_g^-$ state, as originally pointed out by Callomon & Gilby (1963).

Both Callomon & Gilby (1963) and Phillips (1968) listed $N = 31$ and $N = 33$ rotational levels for $v' = 1$ of the $d\ ^3\Pi_g$ state as perturbed. We also confirm this and obtained more accurate shifts (see Table 7 in Appendix A). The $N = 37$ levels for $v' = 1$ are listed as perturbed by Phillips, but not by Callomon & Gilby. Our observation and assignment indicate that these levels are indeed perturbed but the shifts obtained are somewhat different from those given by Phillips.

For the $v' = 2$ level, according to Phillips (1968) $J = 9$, 10, and 11 of the F_2 spin component are perturbed. Our analysis also indicates that these levels are certainly perturbed, but there is an interesting and important difference. The (2, 1) band observed by us is shown in Figure 7 together with the spectra of the (2, 2), (2, 3), and (2, 4) bands. They are displayed by aligning the calculated $R_2(9)$ line positions for these bands. The dotted vertical line indicates the position of the calculated unperturbed transition wavenumbers for the $R_2(9)$ transitions. We identified slightly weaker lines at about 1 cm^{-1} higher to the expected positions. We have assigned these lines as the shifted $R_2(9)$ transitions. The differences between the calculated line positions and observed ones are 0.942, 0.939, 0.954, and 0.951 cm^{-1} for the (2, 1), (2, 2),

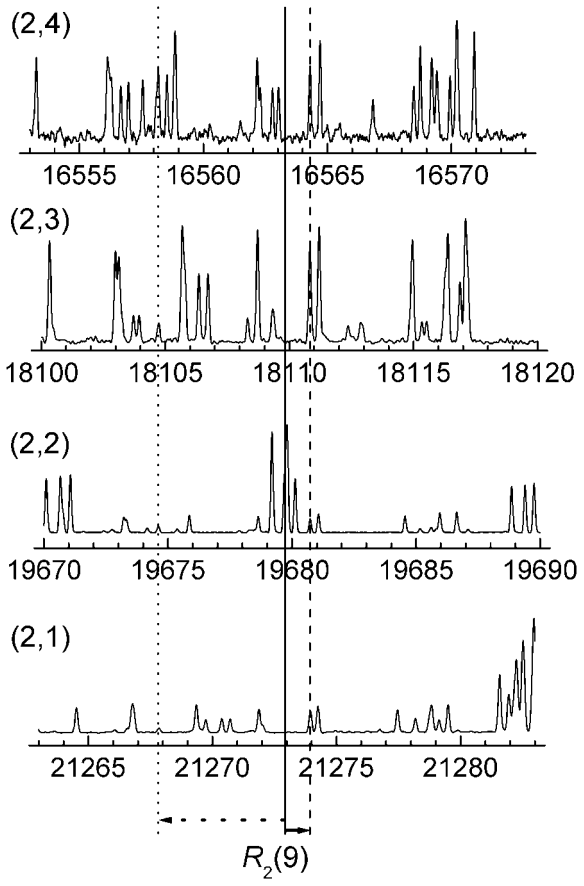

FIG. 7.—$R_2(9)$ transitions for the (2, 1), (2, 2), (2, 3), and (2, 4) bands. The vertical solid line indicates the calculated transition wavenumber for each $R_2(9)$ transition. (The spectra are aligned to the calculated values for the $R_2(9)$ transitions on the same wavenumber scale.) There are no clear intense lines corresponding to the transitions at the expected positions. Instead, relatively strong lines were found with reasonable intensities in their neighborhood at about 1 cm^{-1} higher than the calculated positions (*short-dashed lines*), and the very weak extra lines were also identifiable on the lower wavenumber side (*dotted lines*).

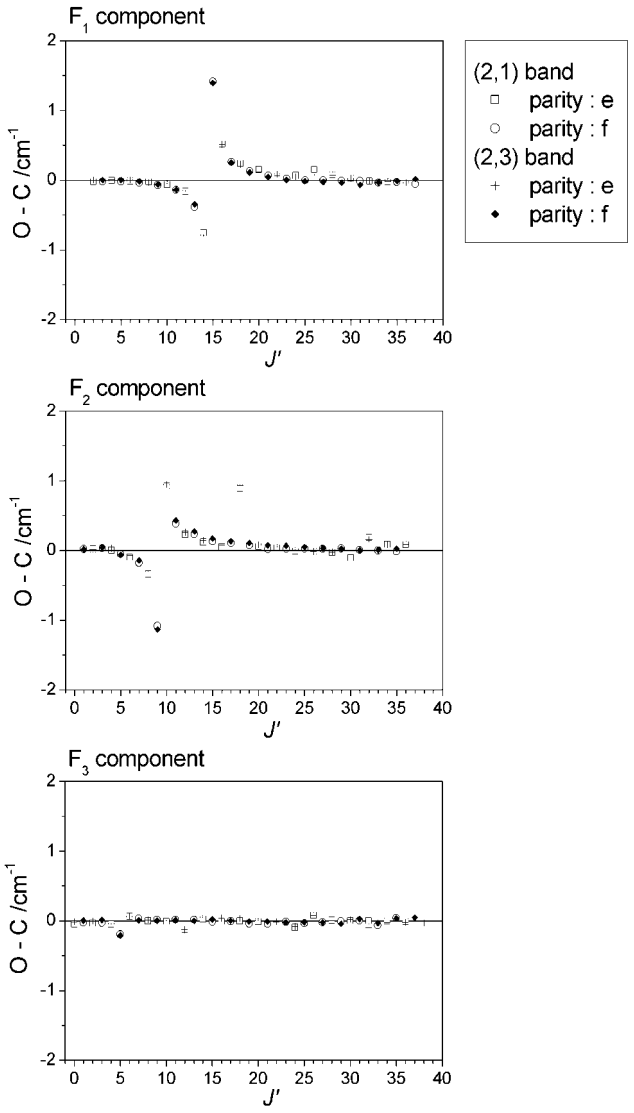

FIG. 8.—Residuals of the fit of the (2, 1) and (2, 3) bands plotted together against the upper state rotational quantum number J'. Each point was obtained from the *R*-branch transitions for each band.

(2, 3), and (2, 4) bands, respectively. These values agree well with each other within experimental error. Therefore, it can be concluded, as Phillips pointed out, that the $J = 10$ level of the F_2 spin component of the $v' = 2$ level is shifted by a perturbation. Similar shifts were found in the corresponding *P*-branch transitions, which confirmed the assignments. In addition, we found much weaker features at the positions indicated by the dotted line at about 5 cm^{-1} lower than the calculated main lines and assigned them as transitions from the perturbing state.

Phillips obtained shifts $(O - C)$ of +1.45, +0.89, and +0.38 cm^{-1} for the $J = 9$, 10, and 11 levels, respectively. The shifts obtained from our analysis are −1.118, +0.949, and +0.413 cm^{-1}, respectively. Our results clearly show that a perturbing state crosses between the $J = 9$ and $J = 10$ levels of the F_2 spin component, and it cannot be a $b\ ^3\Sigma_g^-$ level.

Figure 8 plots the deviations of the transition wavenumbers from the calculated values together for the (2, 1) and (2, 3) bands against the upper rotational quantum number J'. Each point was obtained only from *R*-branch transitions, because the *P*-branch lines were often overlapped by other spectral lines especially in the band head region and this degraded the measurement accuracy. The two sets of residuals of the fit, one for the (2, 1) band and the other for the (2, 3) band, agree well with each other within experimental accuracy. This figure corresponds to Figure 1 of Phillips (1968) but it is clear that our analysis is more reasonable. The transition wavenumbers of these lines together with the deviations are listed in Appendix A for the (2, 0), (2, 1), (2, 2), and (2, 3) bands.

For $^{12}C_2$, only the symmetric states obtained on interchange of the equivalent ^{12}C nuclei are allowed. As a result, only *e*-levels are possible for even-*J* and *f* levels for odd-*J* in the $d\ ^3\Pi_g$ state, and vice versa in the $a\ ^3\Pi_u$ state. In the $b\ ^3\Sigma_g^-$ state, only odd-*N* rotational levels are allowed by nuclear spin statistics. As Figure 8 shows, the deviations caused by the perturbation change smoothly for even- and odd-*J*. Therefore, the $b\ ^3\Sigma_g^-$ state is a very unlikely perturber of these rotational levels in the $d\ ^3\Pi_g$ state. A very likely perturbing state is a high-v level of the $B\ ^1\Delta_g$ state. Phillips also pointed out that the perturbations in the $v' = 2$ level could not be explained by interaction with the $b\ ^3\Sigma_g^-$ state, and he suggested that a high-v level of the ground $^1\Sigma_g^+$ state was a likely perturber. However, in $^1\Sigma_g^+$ states only even-*J* rotational levels are possible, so such smooth deviations over for both the even- and odd-*J* levels are hard to explain.

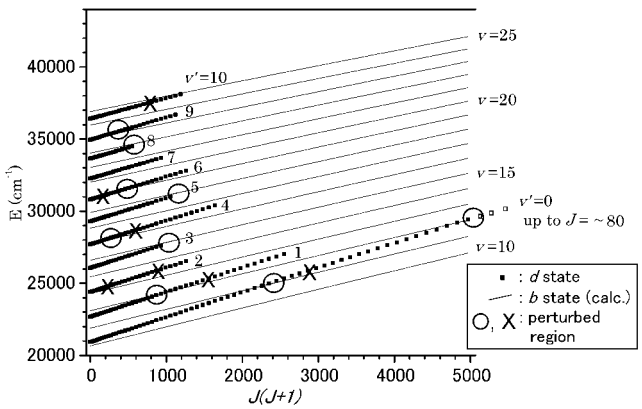

FIG. 9.—Rotational term energies of the $b\ ^3\Sigma_g^-$ (*thin lines*) and $d\ ^3\Pi_g$ (*solid squares*) states.

As now we know that the assignments for the higher v bands by Phillips & Davis (1968) were largely questionable, the discussion on the perturbations in these higher v states given by Phillips needs reconsideration. Most perturbations occur in the upper $d\ ^3\Pi_g$ state, except for the $v = 7$ level of the $a\ ^3\Pi_u$ state, which was discovered in our absorption spectroscopy experiment (Tanabashi & Amano 2002). Rotational perturbations were found in the vibrational levels of $v = 0, 1, 2, 4, 6, 9$, and 10 of the $d\ ^3\Pi_g$ state. The graphical displays of the deviations from the fit for these levels are given in Figure 10 in Appendix B. As various patterns are observed for these deviations, the identification of perturbers and interaction mechanism needs to be considered specifically for each case. We do not go into details in the present paper, but further analysis will be carried out in the future.

Several of the observed perturbations are caused by interactions with the $b\ ^3\Sigma_g^-$ state, which is the upper state of the Ballik-Ramsay system ($b\ ^3\Sigma_g^-$-$a\ ^3\Pi_u$). Callomon & Gilby (1963) extrapolated the term values from the data available at that time (Ballik & Ramsay 1963b) and discussed the perturbations based on such calculated term values. However, the higher v levels, $v \geq 10$, which are supposed to cause the perturbations in the $d\ ^3\Pi_g$ state, have never been observed directly. Amiot et al. (1979) extended the observation of the Ballik-Ramsay system to higher v states up to the (7, 4) band. They derived a set of the Dunham coefficients for both the $b\ ^3\Sigma_g^-$ and $a\ ^3\Pi_u$ states. As this set of molecular constants were determined by including much higher v levels (Amiot et al. 1979), we reevaluated the term values for the $b\ ^3\Sigma_g^-$ state. Figure 9 plots the term values against $J(J + 1)$ for the vibrational levels of the $d\ ^3\Pi_g$ and $b\ ^3\Sigma_g^-$ states. The $d\ ^3\Pi_g$-$b\ ^3\Sigma_g^-$ interactions are marked by hatched blobs, and other perturbations for which the perturbing states are not identified are marked by crosses. It can be seen that the vibrational levels of the $d\ ^3\Pi_g$ and $b\ ^3\Sigma_g^-$ states cross each other at several points. In addition, the high-v levels of the $B\ ^1\Delta_g$ state are also located in the same region, but they are not shown in this figure. Many of the perturbed regions observed in our work are found to be located very close to the $d\ ^3\Pi_g$-$b\ ^3\Sigma_g^-$ crossing points.

TABLE 6

TERM ENERGIES OF THE INTERACTING ROTATIONAL STATES (N) OF $d\ ^3\Pi_g$ AND $b\ ^3\Sigma_g^-$

	$d\ ^3\Pi_g$		$b\ ^3\Sigma_g^-$	
N	v	E (cm^{-1})	v	E (cm^{-1})
47	0	24817. 83	11	24815. 55
69	0	29186. 52	12	29202. 05
31	1	24372. 91	12	24377. 56
35	3	28167. 23	15	28157. 14
9	4	27841. 80	16	27833. 64
37	5	31553. 61	18	31576. 49
19	6	31401. 80	19	31417. 32
31	8	35143. 27	22	35145. 12
15	9	35317. 70	23	35277. 40

Table 6 lists the likely perturbing states for the $d\ ^3\Pi_g$-$b\ ^3\Sigma_g^-$ interactions. This shows that the calculated term values explain very well the perturbations observed most strongly and that these perturbing states are likely to be the high-v' levels of the $b\ ^3\Sigma_g^-$ state. For the unidentified perturbations, it is possible that the vibrationally excited levels of the $B\ ^1\Delta_g$ and $B'\ ^1\Sigma_g^+$ states with appropriate symmetry might be responsible.

5. CONCLUSION

We made an extensive investigation of the bands of the Swan system using a high-resolution Fourier transform spectrometer. We observed the Swan system in emission from a microwave discharge in a mixture of acetylene and argon. A total of 34 bands, up to the (10, 9) band, were identified, and the levels with $v' = 0$–10 and $v'' = 0$–9 were rotationally assigned. Out of these 34 bands, a total of 30 bands were subject to a simultaneous global fit to derive spectroscopic constants. As a result, we found a number of discrepancies between the new measurements and the previous results (Phillips & Davis 1968). In particular, for the high-v bands (higher than $v = 4$) not only disagreements in the measured transition wavenumbers but also misassignments were found. The line assignments and the transition wavenumbers of the six bands involving the levels with $v' = 4$, 5, and 6 are almost completely different from the earlier ones. The Phillips & Davis work is the only previous analysis for such high-v levels of the Swan system. Major sources of this disagreement are thought to be heavy line congestion and many perturbations found in these bands. A study of the perturbations of these states suggests that part of the rotational perturbations are the result of the interactions with high-v levels of the $b\ ^3\Sigma_g^-$ state.

This research was partly supported by the funds from Japan Society for Promotion of Science (JSPS). Support for this work was provided also by the Natural Sciences and Engineering Research Council of Canada and the NASA laboratory astrophysics program.

APPENDIX A

TRANSITION WAVENUMBERS OF THE SWAN SYSTEM.

The assignments and the transition wavenumbers obtained by us are listed in Table 7. Notes:

1. The vacuum wavenumbers in cm^{-1} are listed for the P_1 to R_3 branches with the lower state rotational quantum numbers. The odd J transitions represent the (e)-(e) transitions and the even J transitions the (f)-(f) transitions.

TABLE 7

TRANSITION WAVENUMBERS OF THE SWAN SYSTEM

J''	$P_3(J)$	$O-C$	Note	$R_3(J)$	$O-C$	Note	$P_2(J)$	$O-C$	Note	$R_2(J)$	$O-C$	Note	$P_1(J)$	$O-C$	Note	$R_1(J)$	$O-C$	Note
The (0, 0) Band																		
0.....				19381.784	4	a												
1.....	19373.650	−26	c	19386.556	5	a				19385.141	0	a						
2.....	19370.171	0	a	19391.051	4	a	19372.330	−2	a	19389.152	−1	a				19388.978	3	a
3.....	19367.245	5	a	19396.155	2	a	19369.655	−1	a	19393.294	0	a	19371.762	2	a	19392.523	3	a
4.....	19364.636	7	a	19400.963	3	a	19367.026	−6	a	19397.892	0	a	19369.317	1	a	19396.362	1	a
5.....	19362.473	2	a	19406.367	1	a	19364.846	57	y	19402.615	0	a	19367.026	6	a	19400.487	1	a
6.....	19360.517	3	a	19411.568	1	a	19362.670	1	a	19407.676	0	a	19364.846	−31	c	19404.915	1	a
7.....	19358.970	2	a	19417.337	1	a	19360.944	24	c	19412.903	0	a	19362.974	33	c	19409.629	0	a
8.....	19357.645	83	y	19422.973	0	a	19359.317	2	a	19418.410	0	a	19361.195	1	a	19414.619	2	a
9.....	19356.514	−38	c	19429.154	1	a	19358.029	−33	c	19424.115	0	a	19359.692	2	a	19419.905	3	a
10.....	19355.613	−46	y	19435.244	0	a	19356.949	−11	a	19430.079	0	a	19358.395	8	a	19425.417	2	a

NOTES.—(a) Well-resolved isolated lines; (b) lines with a strange line shape due to overlap with other lines (they are included in the fit with reduced weight); (c) blended lines or lines slightly shifted by perturbations, but included in the fit with reduced weight; (p) extra lines caused by a perturbing state to the $d\,^3\Pi_g$ state; (y) perturbed lines, or most heavily overlapped lines, not included in the fit (however, identifications are certain); (z) perturbed lines, or most heavily overlapped lines, not included in the fit (however, identifications are certain). Table 7 is available in its entirety in the electronic edition of the *Astrophysical Journal Supplement*. A portion is shown here for guidance regarding its form and content.

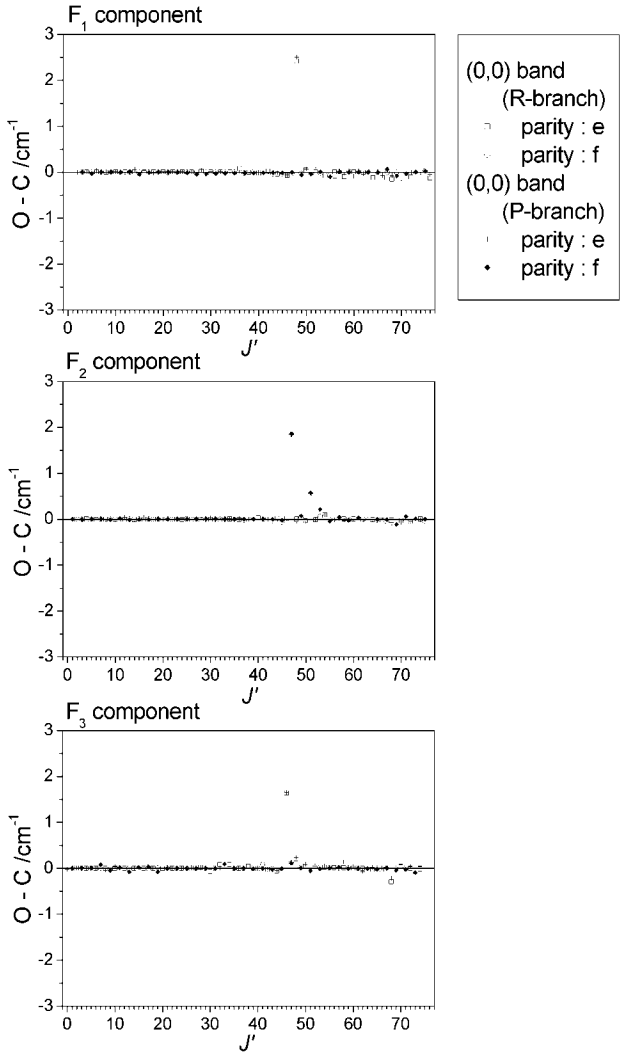

FIG. 10.—Deviations of the rotational energy in $d\ ^3\Pi_g$ for levels (*a*) $v' = 0$, (*b*) $v' = 1$, (*c*) $v' = 4$, (*d*) $v' = 6$, (*e*) $v' = 9$, and (*f*) $v' = 10$. [*See the electronic edition of the Supplement for Figs 10b–10f.*]

2. "$O - C$" indicates the observed minus calculated values times 10^3 in cm^{-1}. $O - C$ is left blank for blended lines that show apparent broadening or shoulder, and the calculated transition wavenumbers are listed.

3. Columns next to the observed minus calculated values are the symbols that categorize the lines as follows: (a) well-resolved isolated lines; (b) lines with a strange line shape due to overlap with other lines (they are included in the fit with reduced weight); (c) blended lines or lines slightly shifted by perturbations, but included in the fit with reduced weight; (p) extra lines caused by a perturbing state to the $d\ ^3\Pi_g$ state; (y) perturbed lines, or most heavily overlapped lines, not included in the fit (however, identifications are certain); (z) perturbed lines, or most heavily overlapped lines, not included in the fit (however, identifications are certain).

APPENDIX B

PERTURBATIONS IN THE $d\ ^3\Pi_g$ STATE

Figure 10 shows deviations of rotational energy in the $d\ ^3\Pi_g$ state for different values of v'.

REFERENCES

Amiot, C. 1983, ApJS, 52, 329
Amiot, C., Chauville, J., & Maillard, J.-P. 1979, J. Mol. Spectrosc., 75, 19
Ballik, E., & Ramsay, D. 1963a, ApJ, 137, 84
———. 1963b, ApJ, 137, 61
Bernath, P. F., & McLeod, S. 2001, J. Mol. Spectrosc., 207, 287
Brault, J. W., Delbouille, L., Gravesse, N., Roland, G., Sauval, A. J., & Testerman, L. 1982, A&A, 108, 201
Brown, J. M., & Merer, A. J. 1979, J. Mol. Spectrosc., 74, 488
Callomon, J. H., & Gilby, A. C. 1963, Canadian, J. Phys., 41, 995
Caubet, P., & Dorthe, G. 1994, Chem. Phys. Lett., 218, 529
Cecchi-Pestellini, C., & Dalgarno, A. 2002, MNRAS, 331, L31
Chaffee, F. H., & Lutz, B. L. 1978, ApJ, 221, L91
Chafee, F. H., Lutz, B. L., Black, J. H., Bout, P. A. V., & Snell, R. L. 1980, ApJ, 236, 474
Chauville, J., Maillard, J. P., & Mantz, A. W. 1977, J. Mol. Spectrosc., 68, 399
Curtis, M. C., & Sarre, P. J. 1985, J. Mol. Spectrosc., 114, 427
Davis, S. P., Abrams, M. C., Phillips, J. G., & Rao, M. L. P. 1988, J. Opt. Soc. Am. B, 5, 2280

Douay, M., Nietmann, R., & Bernath, P. F. 1988, J. Mol. Spectrosc., 131, 261
Erman, P. 1980, Phys. Scr., 22, 108
Federman, S. R., & Huntress, W. T. 1989, ApJ, 338, 140
Fink, U., & Hicks, M. D. 1996, ApJ, 459, 729
Fowler, A. 1910, MNRAS, 70, 484
Goebel, J. H., Bregman, J. D., Cooper, D. M., Goorvitch, D., Langhoff, S. R., & Witteborn, F. C. 1983, ApJ, 270, 190
Gredel, R. 1999, A&A, 351, 657
Gredel, R., Black, J. H., & Yan, M. 2001, A&A, 375, 553
Gredel, R., van Dishoeck, E. F., & Black, J. H. 1989, ApJ, 338, 1407
Grevesse, N., & Sauval, A. J. 1973, A&A, 27, 29
Herzberg, G. 1946, Phys. Rev., 70, 762
Hirao, T., Pinchemel, B., & Bernath, P. F. 2000, J. Mol. Spectrosc., 202, 213
Hobbs, L. M. 1979, ApJ, 232, L175
———. 1981, ApJ, 243, 485
Hobbs, L. M., Black, J. H., & van Dishoeck, E. F. 1983, ApJ, 271, L95
Hobbs, L. M., & Campbell, B. 1982, ApJ, 256, 108
Huber, K. P., & Herzberg, G. 1979, Molecular Spectra and Molecular Structure: Constants of Diatomic Molecules (New York: Van Nostrand Reinhold)
Johnson, J. R., Fink, U., & Larson, H. P. 1983, ApJ, 270, 769
Kunz, C., Harteck, P., & Dondes, S. 1967, J. Chem. Phys., 46, 4157
Lambert, D. L. 1978, MNRAS, 182, 249
Lambert, D. L., & Danks, A. C. 1983, ApJ, 268, 428
Little, C. E., & Browne, P. G. 1987, Chem. Phys. Lett., 134, 560
Lloyd, G. M., & Ewart, P. 1999, J. Chem. Phys., 110, 385
Mayer, P., & O'Dell, C. 1968, ApJ, 153, 951
Norlen, G. 1973, Phys. Scr., 8, 249
Phillips, J. G. 1968, J. Mol. Spectrosc., 28, 233
Phillips, J. G., & Davis, S. P. 1968, The Berkeley Analysis of Molecular Spectra, Vol.2. The Swan System of the C_2 Molecule and the Spectrum of the HgH Molecule (Berkeley: Univ. California)
Prasad, C., & Bernath, P. F. 1994, ApJ, 426, 812
Querci, F., Querci, M., & Kunde, V. G. 1971, A&A, 15, 256
Reddy, B. E., Lambert, D. L., Gonzalez, G., & Yang, D. 2002, ApJ, 564, 482
Savadatti, M. I., & Broida, H. P. 1966, J. Chem. Phys., 45, 2390
Sembach, K. R., Danks, A. C., & Lambert, D. L. 1996, ApJ, 460, L61
Setser, D. W., & Thrush, B. A. 1963, Nature, 200, 864
Souza, S. P., & Lutz, B. L. 1977, ApJ, 216, L49
Suzuki, T., Saito, S., & Hirota, E. 1985, J. Mol. Spectrosc., 113, 399
Tanabashi, A., & Amano, T. 2002, J. Mol. Spectrosc., 215, 285
Tautvaisiene, G., Edvardsson, B., Tuominen, I., & Ilyin, I. 2000, A&A, 360, 499
Tyte, D. C., Innanen, S. H., & Nicholls, R. W. 1967, Identification Atlas of Molecular Spectra, Vol.5. The C_2 $d\ ^3\Pi_g$-$a\ ^3\Pi_u$ Swan System (Toronto: York Univ.)
van Dishoeck, E. F., & de Zeeuw, T. 1984, MNRAS, 206, 383
Weltner, W., Jr., & Van Zee, R. J. 1989, Chem. Rev., 89, 1713

Note added in proof.—The $c\ ^3\Sigma_u^+$ state of C_2 has just been located through observation of the (3, 0) band of the $d\ ^3\Pi_g$–$c\ ^3\Sigma_u^+$ transition (D. L. Kokkin et al., J. Chem. Phys., 125, 231101 [2006]).